Coupling losses in perfluorinated multi-core polymer optical fibers

Gaizka Durana,[1*] Gotzon Aldabaldetreku,[1] Joseba Zubia,[1] Jon Arrue,[1] and Chikafumi Tanaka[2]

[1] *University of the Basque Country, Department of Electronics and Telecommunications Alda. Urquijo s/n, E-48013 Bilbao, Spain*

[2] *Lucina division, Asahi Glass Co., Ltd., 520 Imazato, Susono-shi, Shizuoka 410-1104, Japan*

gaizka.durana@ehu.es

Abstract: The aim of the present paper is to provide a comprehensive analysis of coupling losses in perfluorinated (PF) multi-core polymer optical fibers (MC-POFs), which consist of groups of 127 graded-index cores. In our analysis we take into account geometrical, longitudinal, transverse, and angular misalignments. We perform several experimental measurements and computer simulations in order to calculate the coupling losses for a PF MC-POF prototype. Based on these results, we propose several hints of practical interest to the manufacturer which would allow an appropriate connector design in order to handle conveniently the coupling losses incurred when connectorizing two PF MC-POFs.

OCIS codes: (060.0060) Fiber optics and optical communications; (060.2270) Fiber characterization; (060.2300) Fiber measurements; (060.2310) Fiber optics.

References and links

1. H. Munekuni, S. Katsuta, and S. Teshima, "Plastic Optical Fiber for High-Speed Transmisssion," in *Proceedings of the third international conference on plastic optical fibers and applications-POF'94*, pp. 148–151 (Yokohama (Japan), 1994).
2. "Asahi Glass Product Information," URL http://www.agc.co.jp/english/chemicals/shinsei/cytop/cytop.htm.
3. C. Tanaka, K. Kogenazawa, T. Ohnishi, K. Kurashima, G. Ogawa, M. Sato, N. Ota, and M. Naritomi, "Development of multi-core perfluorinated POF," in *Proceedings of the fifteenth international conference on plastic optical fibers and applications-POF'06*, pp. 152–156 (Seoul (Corea), 2006).
4. D. Gloge, "Offset and tilt loss in optical fiber splices," Bell Syst. Tech. J. **55**, 905–916 (1976).
5. T. C. Chu and A. R. McCormick, "Measurements of loss due to offset, end separation, and angular misalignment in graded index fibers excited by an incoherent source," Bell Syst. Tech. J. **57**, 595–602 (1978).
6. A. W. Snyder and J. D. Love, *Optical waveguide theory* (Chapman and Hall, London, 1983).
7. "Asahi Glass Co., Ltd." URL http://www.agc.co.jp.
8. B. Lohmüller, A. Bachmann, O. Ziemann, A. Sawaki, H. Shirai, and K. Suzuki, "The use of LEPAS System for POF characterization," in *11th international POF conference 2002: Proceedings*, pp. 263–266 (Tokyo (Japan), 2002).
9. "Hamamatsu Photonics," URL http://sales.hamamatsu.com/en/products.php.
10. R. W. Waynant and M. N. Ediger, eds., *Electro-optics handbook*, 2nd ed. (McGraw-Hill, New York, 2000).
11. G. E. Agrawal, *Fiber-optic communication systems*, 3rd ed. (John Wiley & Sons, New York, 2002).
12. D. Marcuse, *Theory of dielectric waveguides* (Academic Press, San Diego, 1974).
13. D. Gloge, "Weakly guiding fibers," Appl. Opt. **10**, 2252–2258 (1971).
14. D. Gloge and E. A. J. Marcatili, "Multimode theory of graded-core fibers," Bell Syst. Tech. J. **52**, 1563–1578 (1973).
15. J. Arrue, G. Aldabaldetreku, G. Durana, J. Zubia, and F. Jiménez, "Computational research on the behaviour of bent plastic optical fibres in communications links and sensing applications," in *Recent research developments in optics*, S. G. Pandalai, ed., vol. 5, chap. 5 (Research Signpost, Kerala (India), 2005).

#91480 - $15.00 USD Received 8 Jan 2008; revised 4 Apr 2008; accepted 28 Apr 2008; published 19 May 2008

16. T. Ishigure, "WKB Method for POF Modelling," in *POF Modelling: Theory, Measurement and Application*, C.-A. Bunge and H. Poisel, ed., (Books on Demand GmbH, Norderstedt (Germany), 2008).
17. J. W. Goodman, *Speckle Phenomena: Theory and Applications*, 1st ed. (Roberts & Company, 2006).

1. Introduction

Multi-core (MC) polymer optical fibers (POFs) constitute an alternative to the traditional and more extended step-index (SI) and graded-index (GI) POFs. The main advantages shown by these fibers [1] are an smaller sensitivity to bending losses than the traditional POFs of large core diameter, and their large size, which makes them particularly suitable for easy handling and light launching.

A new type of MC-POF, made of the perfluorinated polymer called CYTOP ® [2], has been recently presented in a configuration of 127 small GI cores grouped together so that they fill a round cross-section of 350 μm of diameter [3]. Low-cost production is one of the main objectives followed by the manufacturer in order for PF MC-POFs to constitute an attractive and interesting option in next generation Fiber To The Home (FTTH) services in combination with a suitable light source such as a Vertical Cavity Surface-Emitting Laser (VCSEL).

The design of fiber-optical communication systems requires a clear understanding of the limitations imposed by the loss of the fiber. In this sense, it is primary to know the insertion loss of connectors and its dependence on the three fundamental types of misalignments between fibers, namely, longitudinal separation, transverse offset and angular misalignment [4, 5]. In the case of MC-POFs, however, a fourth type of misalignment must be considered, namely the geometrical misalignment, which should be kept under control in order to minimize the coupling losses of these types of fibers.

Previous studies in SI POFs and GI POFs have established that the GI ones are more sensitive to mechanical misalignments than the SI ones, due to the variation of the acceptance cone with the radial position [6]. However, when many cores are grouped together it is more difficult to predict the overall effect of mechanical misalignments on coupling loss. For this reason, it would be very interesting to be able to compare the coupling losses obtained for the PF MC-POFs analyzed in this paper with those obtained for SI MC-POFs. Unfortunately, to the best of our knowledge, there is no study for SI MC-POFs available in the literature, so it is not possible to assess the differences between PF MC-POFs and SI MC-POFs in terms of coupling losses. As a consequence, we will restrict our study to PF MC-POFs.

The structure of the paper is as follows. First, the characteristics of the PF MC-POF are analyzed, in order to justify the use of the geometric ray-tracing method with this type of fiber. Then, the experimental set-up used to measure the coupling losses of PF MC-POFs due to mechanical misalignments is described. After that, the computer simulations are explicated. These computer simulations, based on the ray-tracing method, are carried out with the aim of complementing the experimental measurements and of having a deeper insight into the effects of fiber connection. Next, the experimental measurements as well as the numerical computer simulations of the coupling losses are presented and discussed, to follow with some important considerations for the manufacturer in order to keep the losses as low as possible when connectorizing two MC POFs. Finally, we summarize the main conclusions.

2. Characteristics of the analyzed MC-POF

The PF MC-POF investigated in this paper is an 127-core prototype developed by Asahi Glass [7]. Its most important specifications are summarized in Table 1. In order to determine the geometric arrangement of the 127 cores within the PF MC-POF, we have taken cross-section photographs, as the one shown in Fig. 1.

#91480 - $15.00 USD Received 8 Jan 2008; revised 4 Apr 2008; accepted 28 Apr 2008; published 19 May 2008

Table 1. Specifications of the investigated MC-POF.

	Quantity	Unit
Number of cores	127	–
Core diameter	25	μm
Cladding diameter	350	μm
Area fraction[a]	64.8	%
Numerical aperture	0.185	–
Attenuation[b]	45	dB/km

[a] Area fraction = Core area / (Core area + Clad area).

[b] Measured at 850 nm.

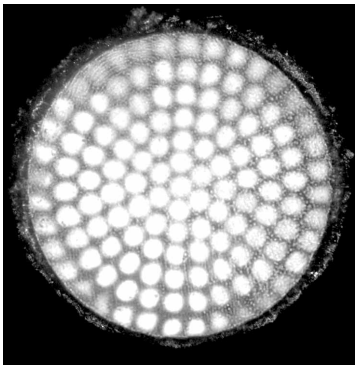

Fig. 1. Cross-section photograph of the investigated PF MC-POF.

Additionally, we have measured the near- and far-fields of the transmitting fiber when illuminating the whole input surface with a green light emitting diode (LED), by using the Hamamatsu LEPAS system [8, 9]. The obtained results, which are discussed in more detail in subsection 5.1, suggest that each core has a parabolic GI profile.

Validity of the geometric optics approach to describe light propagation in MC-POFs

From the characteristics above, we can determine whether each core has a single-mode or multimode behavior. For this purpose, we have to calculate the waveguide parameter or normalized frequency V, which is given by [6]

$$V = \frac{2\pi\rho}{\lambda} NA, \tag{1}$$

where ρ is the core radius, λ is the wavelength of the light in vacuum and NA stands for the maximum numerical aperture. For instance, if we use a wavelength of $\lambda = 850$ nm we obtain $V = 17.094$. This value is higher than the limit value 3.518 for the single-mode condition in a parabolic GI profile [6,10,11], so it can be concluded that the behavior is multimode [6,12–14]. We can also calculate the total number of modes M that can propagate from [14]

$$M \approx \frac{g}{g+2}\frac{V^2}{2}, \tag{2}$$

#91480 - $15.00 USD Received 8 Jan 2008; revised 4 Apr 2008; accepted 28 Apr 2008; published 19 May 2008

where the factor g is the so-called profile exponent. For the previously considered wavelength, and for a parabolic profile ($g = 2$), this value turns out to be $M \approx 73$, which indeed suggests that each core supports a significant amount of modes. Therefore, it is possible to analyze this kind of fiber by using a geometric ray-tracing method [6]. Note that we can extend this conclusion to the visible region of the electromagnetic spectrum, since it involves shorter wavelengths of light and, consequently, a higher number of modes inside each core. Therefore, it is also safe to apply the geometric optics approach in the case of the green LED discussed in the following section.

3. Experiment

Figure 2 shows the experimental set-up employed to measure the coupling losses of PF MC-POFs due to mechanical misalignments.

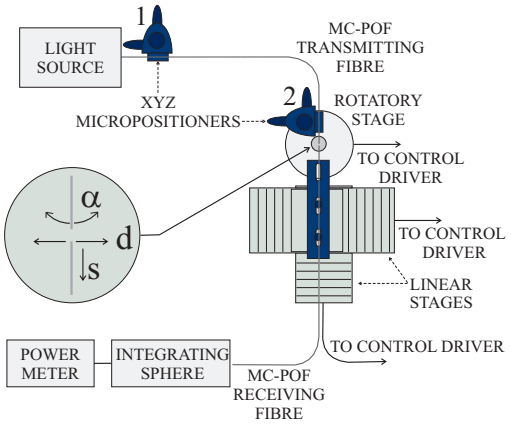

Fig. 2. Experimental set-up used to measure coupling losses of PF MC-POFs.

The receiving fiber is fixed to one of the two linear stages which are placed perpendicularly to each other, whereas the transmitting fiber stands on a rotatory stage. Additionally, the transmitting fiber can be rotated around its symmetry axis. The system is fully automated, and it allows the measurement of angular misalignments, longitudinal separations and transverse offsets, as well as geometrical misalignments. In all the measurements, the length of both the transmitting and receiving fibers was 2 m.

The measurements have been performed using different configurations for the light source: (1) a green LED, and (2) a red laser diode ($\lambda = 662.5$ nm) positioned in front of a pinhole and a microscope objective ($A10/0.25$), which allows us to select one out of three possible numerical apertures at the input surface of the transmitting fiber: $NA_{input} = 0.038$ ($\phi_{\text{pinhole}} = 1$ mm), 0.11 ($\phi_{\text{pinhole}} = 3$ mm), or 0.25 (without pinhole). Notice that the variation of the numerical aperture with the wavelength of light is practically negligible in the visible region of the electromagnetic spectrum, and, therefore, the choice of the wavelength is not relevant in the analysis of coupling losses.

In the case of the green LED, the spot size covers completely the input surface of the transmitting fiber, whereas in the other set-ups of the light source the laser spot size is much smaller than the fiber diameter. This spot size ranges between a full width at half maximum (FWHM) of 2.55 μm and one of 38.39 μm. These two values are obtained with an input numerical aperture of 0.25 and 0.038, respectively. Both the spot size and the numerical aperture have been measured from the near- and far-field patterns of the transmitting fiber by using the Hamamatsu

#91480 - $15.00 USD Received 8 Jan 2008; revised 4 Apr 2008; accepted 28 Apr 2008; published 19 May 2008

LEPAS system [9]. This system allows a very precise control of the input conditions at the entrance of the transmitting fiber (i.e., the numerical aperture and the spot size), which ensures the repeatability of the measurements. The light that exits the receiving fiber is collected by an Ulbricht integrating sphere.

Each of the measurements began by establishing the position $d = s = \alpha = 0$, i.e. that when the transmitting and receiving fibers are aligned. The alignment process was carried out by means of an imaging system consisting of a CCD camera and a magnifying optical system placed vertically just above the transmitting and receiving fibers.

Therefore, for each of the light source configurations described above, the coupling loss measurements were carried out sequentially as follows: first of all, the near- and far-fields of the transmitting fiber were measured by means of the aforementioned LEPAS system. After that, coupling loss against longitudinal separation measurements were taken for different polar angles of the transmitting fiber, which account for the geometrical misalignments in MC-POFs. The polar angle describes the angular orientation of the fiber with respect to a fixed reference direction defined in the plane perpendicular to the fiber axis; for example, if we take a Cartesian coordinate system in which **z** is the axial direction, the polar angle is measured counterclockwise with respect to the fixed *x* axis in the transverse *xy* plane. Figure 3 shows graphically the definition of the polar angle.

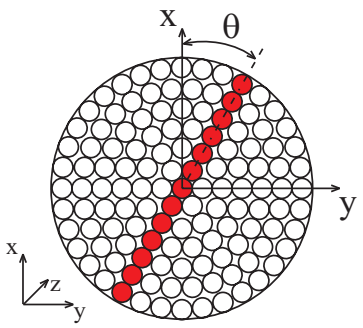

Fig. 3. Definition of the polar-angle misalignment.

Similarly, coupling loss against measurements of longitudinal separation were recorded for different transverse offsets. Next, coupling loss against measurements of transverse offset were taken, but this time for different longitudinal separations; and, finally, coupling loss against angular misalignment was measured. The step size for each set of measurements was different: 50 μm for longitudinal separation, 20 μm for transverse offset, and 0.5 $^\circ$ for angular misalignments. Each measurement was repeated three times and the mean value was taken in order to obtain more accurate experimental results. For convenience, the results of coupling loss will be represented using each misalignment parameter normalized with respect to the radius of the cladding (where applicable).

4. Simulation

In order to obtain full knowledge of the effects of fiber connection on light transmission, the experimental measurements have been complemented by computer simulations. It is important to stress on the fact that the simulation results are intended as a first approach, because of the simplifying hypotheses we have made. Firstly, we have considered the cladding region between individual cores as a completely absorbing media, i.e. all rays that refract into this region are absorbed immediately. As a consequence, our computer model neglects the crosstalk between

#91480 - $15.00 USD Received 8 Jan 2008; revised 4 Apr 2008; accepted 28 Apr 2008; published 19 May 2008

adjacent cores. And, secondly, any mode coupling effect inside each individual core has been neglected.

The first simplification is fundamental and necessary, because, otherwise, the implementation of a computer model based on the ray-tracing method would be very elaborate and complicated. As we will see in the following section, when the light source is the laser diode, the crosstalk is too important to be neglected, which limits considerably the applicability of the computational simulations. Nevertheless, we can still make use of the results obtained from these computational simulations for the green LED, since they can still provide interesting information about the effects involved in fiber connection. This is so because the effects of crosstalk are not so influential when the light source covers the entire input surface of the transmitting fiber.

The second assumption has been made on the basis that a selective launch of modes in each GI core gives rise to a near-field pattern that depends on the order of the mode, which suggests a weak mode coupling between adjacent modes [16]. This fact can be observed in the far-field patterns shown in the following section (see Figs. 4(b), 5(b), 5(d) and 5(f)), where the different angular emission patterns suggest a low mode coupling. The different far-field patterns correspond to different launching conditions, as explained in section 3.

Let us now describe the hypothetical light source that we have employed in our simulations for the case of the green LED. It has been designed in such a way that the computational near-field pattern obtained at the output surface of the transmitting fiber resembles the corresponding experimental near-field pattern. This design enables us to compare the numerical results with the experimental ones. Regarding the emission characteristics, we have used a Lambertian green LED that covers the whole surface of the transmitting fiber, the Lambertian exponent s being 1.0. We have launched a high enough number of rays into the PF MC-POF (more specifically, 315000) to ensure sufficiently smooth and accurate results [15].

The step size considered for the different sets of simulations is smaller than the corresponding values used in the experimental measurements: 10 μm for longitudinal separation, 5 μm for transverse offset, and 0.05° for angular misalignment. It should be noticed that, in the graphical representation of the numerical results, part of the line-symbols have been dropped for the sake of clarity.

5. Results and discussion

5.1. Near- and far-field patterns

Figures 4 and 5 show the experimental near- and far-field patterns measured at the output surface of the transmitting fiber for different launching conditions. Each near-field pattern represents the emission pattern of the corresponding light source filtered by the local numerical aperture of the MC-POF and modified by the crosstalk between adjacent cores. Figure 4 corresponds to the case of the green LED and Fig. 5 to the case of exciting the transmitting fiber with the three different numerical apertures.

Additionally, we have plotted on Fig. 6 the corresponding simulated near- and far-field patterns for the green LED.

The reader is cautioned that the simulations do not take into account the speckle phenomenon of the laser diode, a type of high-contrast, fine-scale granular pattern of the light spot originated by the coherent nature of the laser source [17]. This effect can be observed by the rather irregular shape of the experimental far-field patterns observed in Figs. 5(b), 5(d) and 5(f).

5.2. Longitudinal separation

In order to observe the influence on coupling losses of the geometrical misalignment caused by a different polar angle, we present below both the experimental and numerical results for the coupling losses (in dB units) against the normalized longitudinal separation s/a corresponding

#91480 - $15.00 USD Received 8 Jan 2008; revised 4 Apr 2008; accepted 28 Apr 2008; published 19 May 2008

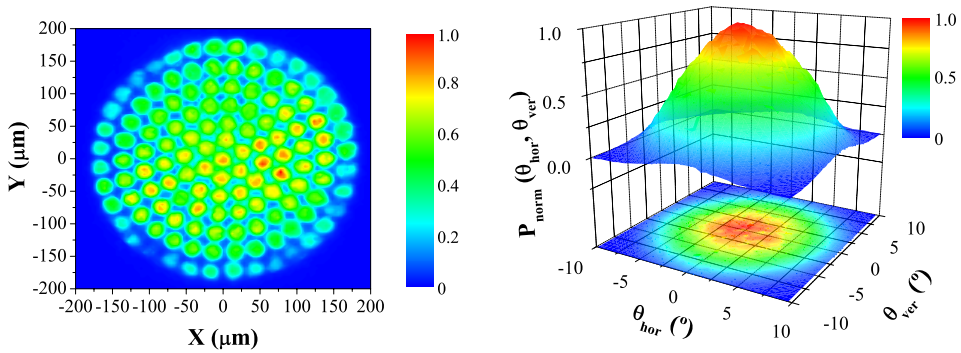

(a) Near-field for a green LED.

(b) Far-field for a green LED.

Fig. 4. Experimental near- and far-fields of the investigated PF MC-POF for a green LED. Both power distributions have been measured at the exit of the transmitting fiber.

to different polar angles θ of the transmitting fiber ($a = 175$ μm denotes the radius of the cladding). Figure 7 shows the results corresponding to the green LED source.

It can be seen that the numerical results show, in general, fairly pessimistic values, in contrast to the experimental ones (due to the assumption of a completely absorbing media for the cladding region and the absence of mode coupling between adjacent cores). Nevertheless, even though the results obtained from these simulations are intended as a first approach, the similar tendencies shown by both the experimental and numerical results make it possible to compare them qualitatively (the computational simulations serve as a complement to the experimental measurements).

Let us now focus the discussion on the qualitative behavior of the experimental and numerical results shown in Fig. 7. It is worthy of note that, in both cases, the coupling losses depend strongly on the polar angle for small longitudinal separations ($s/a \lesssim 1.2$) or even in the absence of longitudinal separation. In fact, the greatest difference in the coupling losses in the figure occurs when no longitudinal separation exists. This is so because, if the receiving fiber is rotated about the axial direction, the different cores of both fibers do not couple correctly together (even in the absence of any other mechanical misalignment). It is important to note that we do not encounter such an additional source of losses in standard one-core fibers. This is due to the azimuthal symmetry exhibited by these fibers. This suggests that, for small longitudinal separations, the coupling losses depend on the near-field pattern of the transmitting fiber.

In view of the acute sensitivity of coupling losses to the geometrical misalignment for small longitudinal separations, let us analyze the coupling loss as a function of the polar-angle misalignment in the absence of any other mechanical misalignment ($s = d = \alpha = 0$) and for the green LED. Although we did not carried out the corresponding experimental measurements, we can still make use of the computer simulations to obtain valuable information and draw meaningful conclusions. This is shown in Fig. 8. It is worthy of note the great dependence of coupling losses on the polar angle when the green LED is involved. The computer simulations, therefore, help us to realize the importance of the polar-angle misalignment in the coupling losses.

If we now return again to Fig. 7, we can observe that, for sufficiently large longitudinal separations ($s/a \gtrsim 1.2$) the dependence of coupling losses on the polar angle disappears, which is indicative that coupling losses now depend on the gaussian-shaped far-field pattern of the transmitting fiber.

#91480 - $15.00 USD Received 8 Jan 2008; revised 4 Apr 2008; accepted 28 Apr 2008; published 19 May 2008

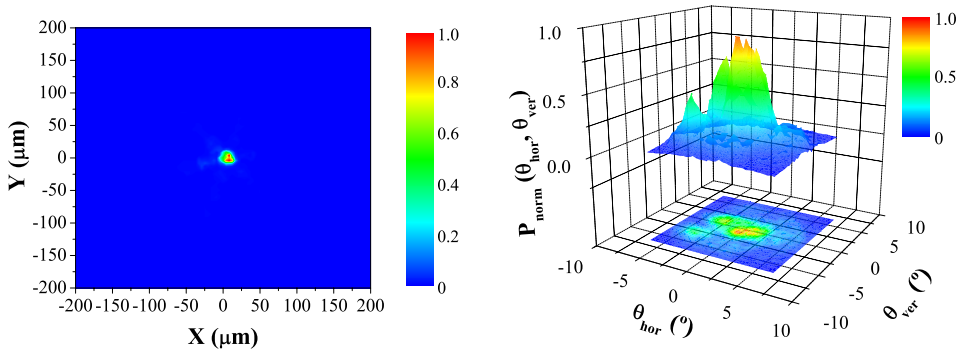

(a) Near-field with $NA_{input} = 0.038$. (b) Far-field with $NA_{input} = 0.038$.

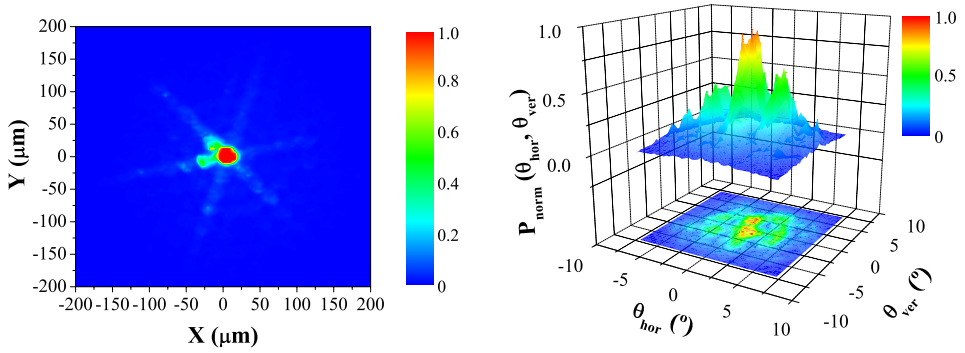

(c) Near-field with $NA_{input} = 0.11$. (d) Far-field with $NA_{input} = 0.11$.

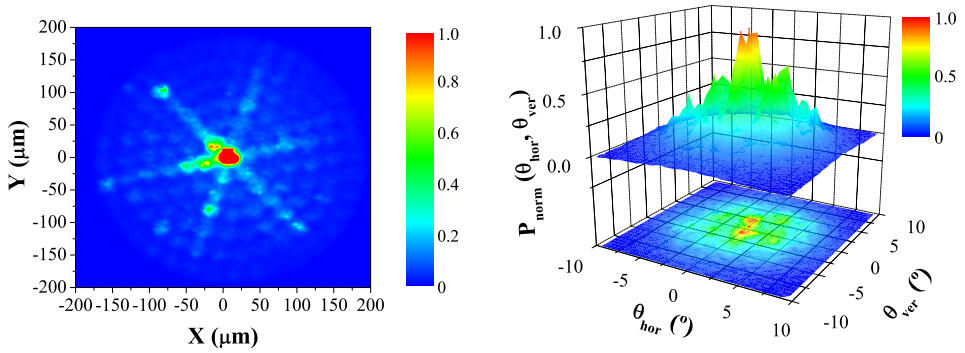

(e) Near-field with $NA_{input} = 0.25$. (f) Far-field with $NA_{input} = 0.25$.

Fig. 5. Experimental near- and far-fields of the transmitting fiber for the sources of different numerical aperture.

#91480 - $15.00 USD Received 8 Jan 2008; revised 4 Apr 2008; accepted 28 Apr 2008; published 19 May 2008

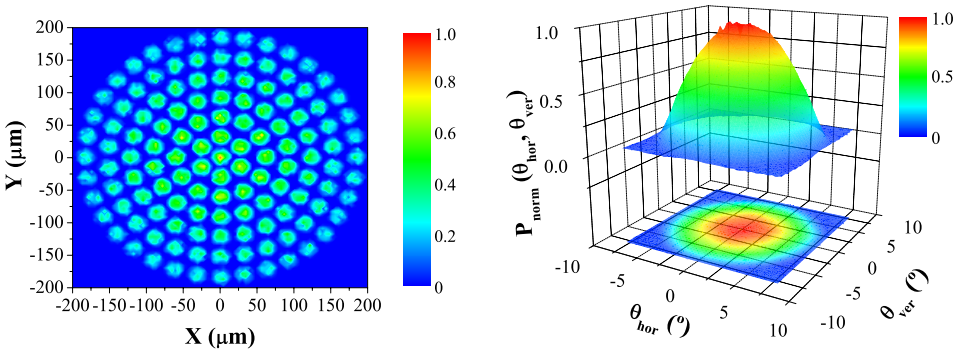

(a) Near-field with a green LED. (b) Far-field with a green LED.

Fig. 6. Near- and far-fields of the transmitting fiber for the green LED used in the numerical computer simulations.

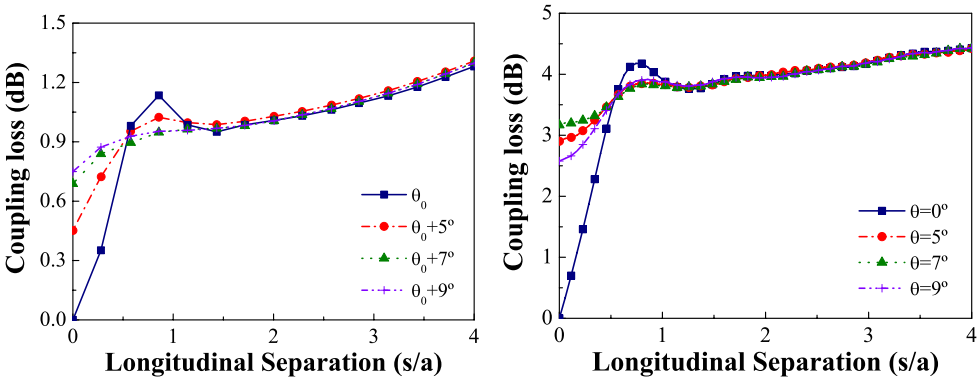

(a) Experimental results with a green LED. (b) Numerical results with a green LED.

Fig. 7. Dependence of coupling losses on the polar angle misalignment of the investigated PF MC-POF for a green LED. θ_0 denotes an arbitrary polar angle of the transmitting fiber.

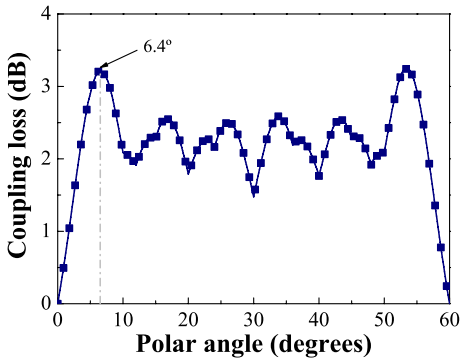

Fig. 8. Coupling loss against polar angle misalignment in the absence of any other mechanical misalignment for the green LED. The value in degrees indicate the polar-angle where the coupling loss is maximum.

#91480 - $15.00 USD Received 8 Jan 2008; revised 4 Apr 2008; accepted 28 Apr 2008; published 19 May 2008

With regard to the other light source configurations ($NA_{input} = 0.038$, $NA_{input} = 0.11$ and $NA_{input} = 0.25$), the coupling losses have the same behavior with the polar angle, namely they depend on the near-field pattern for small longitudinal separations, and on the far-field pattern for sufficiently large longitudinal separations.

Figure 9 shows the experimental and numerical results obtained for the coupling losses as a function of the normalized longitudinal separation s/a for different transverse offsets when the green LED is used.

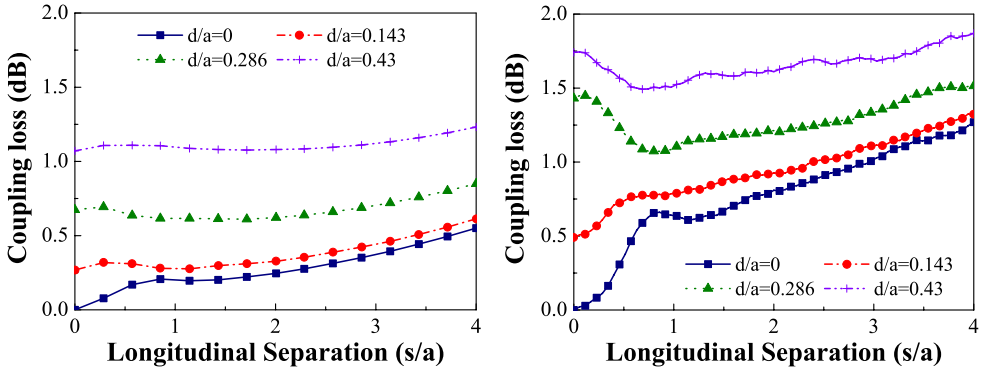

(a) Experimental results. (b) Numerical results.

Fig. 9. Coupling loss against normalized longitudinal separation s/a for various transverse offsets and for a green LED. Experimental and numerical results.

Figure 10 shows the same type of results for light sources of uniform mode distribution with different numerical apertures ($NA_{input} = 0.038$, 0.11 and 0.25), but in this case, all the results are experimental.

For each light source, the measurements have been carried out at a fixed polar angle of the transmitting fiber. This polar orientation has been chosen in such a way that the variation of coupling losses between the minimum and maximum longitudinal separations be minimum. Note that the 0-dB reference point is fixed at this polar angle, because the effects of the geometrical misalignment were not taken into account when the experimental measurements were carried out. Nevertheless, we can make use of the information provided by the computational simulations in Fig. 8 to see the consequences of choosing the polar orientation in this way. It turns out that, at the chosen polar angle, coupling losses due to the geometrical misalignment are maximum when no other type of mechanical misalignment is present (for the green LED, this polar angle turns out to be $\theta_{chosen} = 6.4^{\circ}$). Therefore, caution must be taken when interpreting the obtained results.

Let us first compare the experimental and numerical results (for the green LED) shown on Figs. 9(a) and 9(b), respectively. It is important to keep in mind that the fairly pessimistic values shown by the numerical results are due to the assumption of a completely absorbing media for the cladding region. However, we can use these numerical results as a complement to the experimental ones, because they provide additional information about the dependence of coupling losses on the fiber structure. Indeed, the finer step size of the numerical measurements allows us to observe in the results the characteristic ripples inherent to the multi-core nature of these fibers, whereas this behavior is not easily distinguishable in the experimental results.

Regarding the dependence of the coupling losses on the input numerical aperture (refer to Figs. 10(a), 10(b) and 10(c)), it is surprising to observe that these do not increase with the input numerical aperture. This fact can be understood from the near- and far-fields corresponding to

#91480 - $15.00 USD Received 8 Jan 2008; revised 4 Apr 2008; accepted 28 Apr 2008; published 19 May 2008

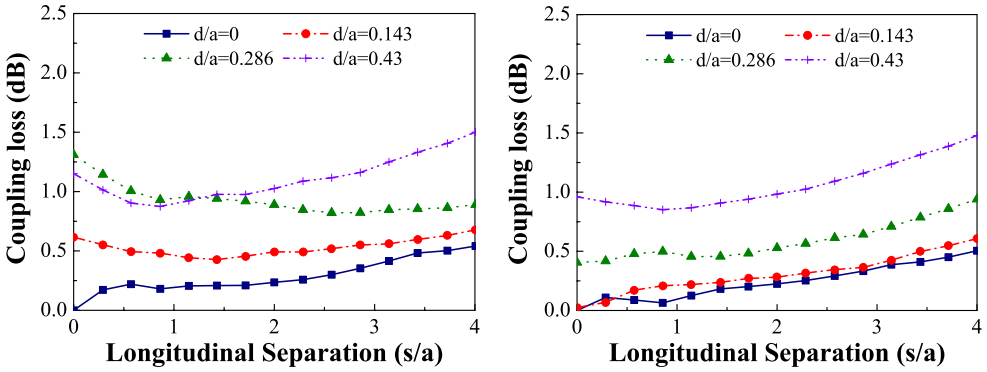

(a) Experimental results with $NA_{input} = 0.038$.

(b) Experimental results with $NA_{input} = 0.11$.

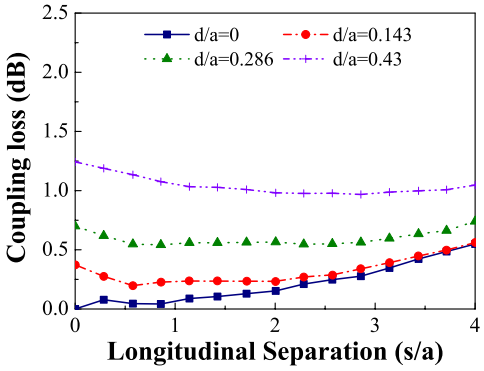

(c) Experimental results with $NA_{input} = 0.25$.

Fig. 10. Coupling loss against normalized longitudinal separation s/a for various transverse offsets and for sources of different numerical aperture.

our light sources of several NA. For instance, Figs. 5(c) and 5(d) show that most of the energy is concentrated in the central cores, in such a way that, at the exit of the transmitting fiber, the cross-section of the radiation pattern is narrow in its base (at $s = 0$) and, therefore, the transmitting fiber is not able to radiate outside the input surface of the receiving fiber.

5.3. Transverse offset

Next we show the results obtained for the coupling loss as a function of the normalized offset d/a for different longitudinal separations and source configurations.

First of all, both in Fig. 11 (green LED source) and in Fig. 12 (different NA light sources) it can be seen that even small offsets result in high coupling losses in comparison with those caused by the longitudinal separation. In fact, it can be observed that the longitudinal separation only has a little effect on the coupling loss, since, in most cases, the different curves in each graph almost overlap.

In the case of light sources of different *NA*, coupling losses increase steadily for moderate normalized transverse offsets. If the transverse offset is large enough for the central GI cores of the transmitting fiber (which carry most of the energy) to be able to radiate outside the input surface of the receiving fiber, there is a significant increase in the coupling loss.

It is particularly interesting that the numerical results in Fig. 11(b) show fluctuations in the

#91480 - $15.00 USD Received 8 Jan 2008; revised 4 Apr 2008; accepted 28 Apr 2008; published 19 May 2008

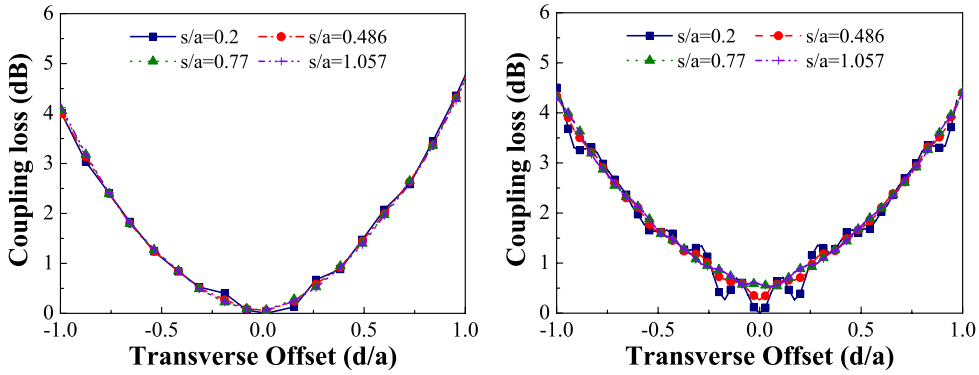

(a) Experimental results. (b) Numerical results.

Fig. 11. Coupling loss against normalized transverse offset d/a for various longitudinal separations and for a green LED. Experimental and numerical results.

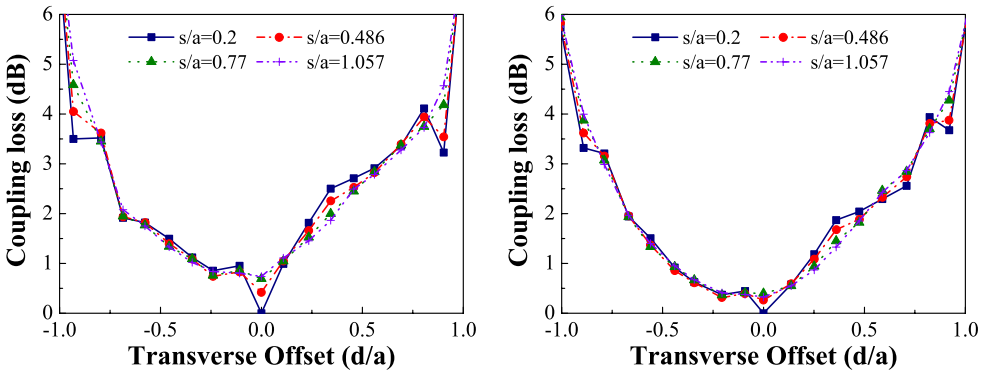

(a) Experimental results with $NA_{input} = 0.038$. (b) Experimental results with $NA_{input} = 0.11$.

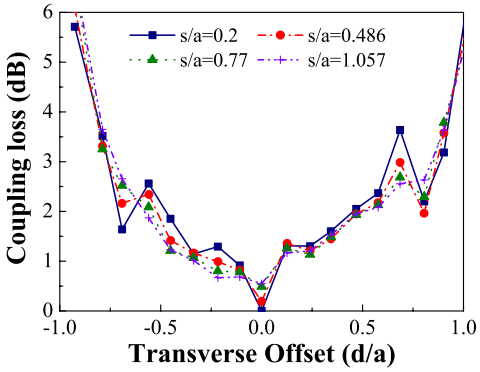

(c) Experimental results with $NA_{input} = 0.25$.

Fig. 12. Coupling loss against normalized transverse offset d/a for various longitudinal separations and for sources of different numerical aperture.

#91480 - $15.00 USD Received 8 Jan 2008; revised 4 Apr 2008; accepted 28 Apr 2008; published 19 May 2008

coupling loss. This oscillatory behavior can be understood by taking into account that the degree of overlapping between individual cores of the transmitting and receiving fibers changes with the transverse offset. In contrast, in the experimental results (Figs. 11(a), 12(a), 12(b) and 12(c)) these variations are partially masked. The reason for this fact is two-fold. On the one hand, the step size for the experimental measurements is not small enough to be able to notice the ripples in the coupling loss. On the other hand, the cladding region also guides part of the light power, since it not lossy enough (in fact, this guiding promotes crosstalk between adjacent cores).

It is also remarkable that, for a fixed small transverse offset, the coupling losses do not increase with the input numerical aperture. This could be explained again by the fact that the light power exiting the transmitting fiber is mainly concentrated within the central region so, for small transverse offsets, even if the aperture of the cone of radiation increases with the input numerical aperture, most of the light exiting the transmitting fiber is still coupled into the receiving fiber.

It is worthy of mention that the lack of azimuthal symmetry of the PF MC-POF gives rise to an additional dependence of the coupling loss on the direction of movement in the transverse plane. In the numerical simulations the transverse offset has always been applied along the y axis (see Fig. 3), whereas this direction was not measured in the experimental case. The probable lack of coincidence between both directions results in an additional factor that contributes to the small quantitative discrepancies observed between the experimental and numerical results for the green LED.

5.4. Angular misalignment

Figure 13 shows the experimental and numerical results of coupling losses as a function of the angular misalignment for the green LED.

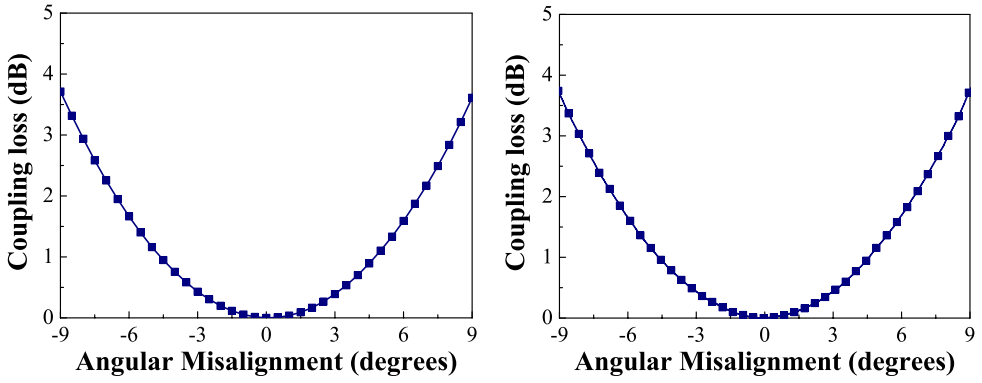

(a) Experimental results. (b) Numerical results.

Fig. 13. Coupling loss against angular misalignment α (in degrees) for a green LED. Experimental and numerical results.

The measured output power refers to the power recorded when $d/a = 0$, $s/a = 1$ and $\alpha = 0$. This is the 0-dB reference point.

It can be observed that the experimental and numerical results corresponding to the green LED agree satisfactorily. Regarding the other light sources, with which the input numerical aperture is 0.038, 0.11 and 0.25, the obtained results are practically the same as those in the case of the green LED and, therefore, they are not shown here. As a consequence, we can conclude that the coupling losses due to an angular misalignment do not depend on the input

#91480 - $15.00 USD Received 8 Jan 2008; revised 4 Apr 2008; accepted 28 Apr 2008; published 19 May 2008

numerical aperture. This fact can be explained on the basis of the geometry of the PF MC-POF and of the light distribution at the output of the transmitting fiber.

In general, it can be concluded that the angular misalignment is not as critical as the transverse offset, provided that it is kept sufficiently small ($\alpha \leq 3^\circ$).

Finally, it is important to remember again that coupling losses depend on the polar angle. For this reason the experimental and numerical results shown in Fig. 13 do not necessarily correspond to the same polar angle because there is a lack of knowledge about the experimental polar angle. All in all, this quantitative discrepancy is practically negligible for small angular misalignments.

5.5. Important considerations for the manufacturer regarding the polar misalignment

Let us now focus on the green LED so as to draw some important conclusions of great interest for any manufacturer interested in maintaining the losses as low as possible when connectorizing two MC POFs.

We will refer again to Fig. 8, which shows the numerical results of the coupling losses as a function of the polar-angle misalignment in the absence of any type of mechanical misalignment. It can be seen that the maximum value of the curve corresponds to the polar angle of 6.4°, giving rise to a coupling loss higher than 3 dB. It is necessary to keep the polar angle as small as 1.7° in order to ensure that coupling losses are never higher than 1 dB. In view of these results, for minimizing the coupling losses incurred when connectorizing two PF MC-POFs, a key factor is to keep under control the geometrical misalignment between the transmitting and receiving fiber. This goal could be achieved, in practice, by printing a narrow colored stripe on the buffer of the fiber representing the reference polar angle ($\theta = 0$). This stripe would be useful to designers for designing a connector in which the geometrical misalignment between the transmitting and receiving fiber can be conveniently controlled.

6. Conclusions

In this paper we have measured coupling losses experimentally using different light sources. In the case of a green LED, we have compared the experimental results with those obtained from numerical simulations. We have observed that the numerical discrepancies observed between the numerical simulations and the experimental data are motivated by the simplifications we have had to make in order to be able to implement our computational model based on the ray-tracing method. Apart from the usual mechanical misalignments (longitudinal separation, transverse offset and angular misalignment) that are present in any kind of fiber, in the case of MC-POFs the geometrical misalignment between the transmitting and receiving fibers is an additional issue to keep in mind in order to minimize coupling losses. For this reason, it would be a good idea to print a narrow stripe on the buffer of the MC-POF that would made the connector designer aware of the geometrical disposition of the individual cores. Finally, in view of the obtained results, the geometrical misalignment and the transverse offset are the most critical parameters from the point of view of coupling losses.

Acknowledgments

The authors would like to thank Prof. H. Poisel of the University of Applied Sciences of Nuremberg for many fruitful discussions.

This work was supported by the institutions *Ministerio de Educación y Ciencia*, *Universidad del País Vasco/Euskal Herriko Unibertsitatea*, *Gobierno Vasco/Eusko Jaurlaritza*, and *European Union 7th Research Framework Programme*, under projects TEC2006-13273-C03-01, GIU05/03 and EJIE07/12, HEGATEK-05 and SHMSENS, and AISHAII, respectively.

#91480 - $15.00 USD Received 8 Jan 2008; revised 4 Apr 2008; accepted 28 Apr 2008; published 19 May 2008